IAC-03-A.5.03

Star Sensor Algorithm Application and Spin-Off

M. Kruijff*, E.J. v.d. Heide*, C.W. de Boom+, N. v.d. Heiden+

* Delta-Utec Space Research and Consultancy, Leiden, the Netherlands, www.delta-utec.com
TNO-TPD, Delft, the Netherlands, www.tpd.tno.nl

Abstract

Many star sensor developments are currently ongoing, varying from high to medium range of accuracy. Modern imaging hardware allows for development of low-cost sensors for small satellites, that can now compete with much less accurate traditionally cheaper systems. This has been the incentive for development of generic tool to assist design and verification of star sensor hardware and algorithms: the SSATT or Star Sensor & Algorithm Test Tool. Performance is measured in obtainable attitude accuracy, reliability, database size.
To allow for a quantification of performance and competitive comparison of results, new algorithms have been developed for automated on-board database construction, pointer based database search, star triangle recognition and validation techniques.
The SSATT algorithms have been tested against leading existing algorithms (Liebe, Quine, Van Bezooijen) and show excellent performance. Also the users' recognition algorithms can be readily coupled via a dll to the Monte Carlo tool for performance comparison.
Algorithms for detection and centroiding and their optimization for a specific camera or lens were developed and allow for a direct connection between real hardware and the SSATT algorithms.
A demo version is available, contact ssatt@delta-utec.com or see the web-site www.delta-utec.com.

The tool has been very successfully applied to images from the MEFIST-II star sensor ground-tested by TNO-TPD in the Negev desert.
The algorithm code has now been redeveloped and optimized in C++ for embedded and flight systems.

Tests have indicated that the SSATT algorithms can also be used on-ground with medium-grade CCD or CMOS sensors with large field of view. This allows for a variety of spin-off applications as detailed in this paper. The database storage and retrieval algorithm has been successfully transferred to a medical application.

This paper describes the functionality of the SSATT, discusses the algorithms and tests performed and possibilities for spin-off development.

1. SSATT functionality

The Star Sensor & Algorithm Test Tool (SSATT) is a tool for:

- Star sensor camera hardware development (requirements definition, performance estimation etc.).
- Star sensor algorithm development (test bed via dll interface).
- Assessment of performance of real-sky imagery.
- Variety of spin-off applications

A full set of advanced algorithms has been developed for SSATT, that have shown to be very generic and can be used with any star sensor as well as with many ground applications.

Major functionality:

- Star catalogue conversion (selection of suitable stars, conversion from visual to instrumental magnitude)
- Automated star-triangle database production for embedded (flight) system (on-board database)
- Unique database organization for immediate star identification with (near-) zero search time
- Input of real images or fast graphic simulation of camera images (for Monte Carlo simulation of the full sky, including camera-specific noise, Fig. 1.1)
- Star detection/centroiding
- Star-triangle recognition and validation algorithms
- QUEST attitude determination

Further features:

- Dealing with complications such as optical-binary stars, false star rejection etc.
- Genetic algorithm optimization of lens projection
- Interface with TNO-TPD developed synthetic image generator (noisy star pixel maps)
- Flight software version (embedded system C++ code) of the image processing, star identification and attitude determination

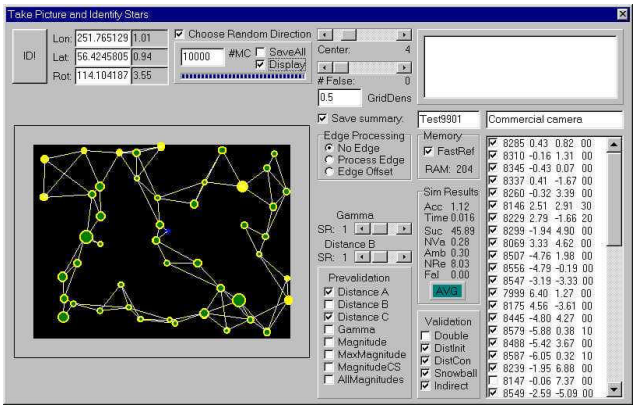

Fig. 1.1 SSATT Image Recognition Screen

2. Algorithms of SSATT

This section gives a brief overview of the star identification algorithms that are explained in detail in [Ref. 2], as well as the detection, rejection and centroiding algorithms.

In SSATT, the star recognition from a CCD image is performed by extracting, for each star to-be-identified, a combination of features of a triangular pattern.

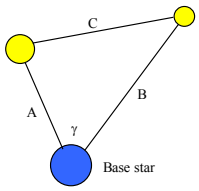

Fig. 2.1: A triangle pattern plus feature definitions

Useful features must be independent from the camera attitude and can thus be a magnitude or a great-circle angular distance between two stars (see Fig. 2.1).
In SSATT, any combination of the above can be used for identification. When a triangle pattern's features have been measured in the image, a database is searched for a very similar pattern that is used for identification. Using a pointer based search strategy and a uniformized database, all candidate triangles are located in a single step, completely independent of the database size.
After recognition, to achieve the required reliability, the candidate identifications need to be filtered through a validation algorithm. Various algorithms are available.
With a group of stars identified, the Star Sensor Algorithm Test Tool applies the QUEST algorithm[4,5] to obtain an attitude estimate and investigate performance.

2.1 Development of On-board Database for Triangle recognition

The key part of the autonomous star sensor S/W is the on-board database and its structure to facilitate efficient triangle pattern search. The database has to be created on-ground by the following steps, which are automated in SSATT:

- Conversion of star magnitudes from catalogued visual value to instrumental magnitude;
- Selection of best triangles to be stored;
- Calculation, organization and uniformization of triangle features for storage.

2.1.1 Conversion of star magnitudes and star catalogue

A database of stars needs to be produced from the instrumental magnitude of the catalogued stars. However, the magnitude of stars is catalogued in *visual* frequency domain. Such a magnitude can differ up to 2 from the magnitude as observed by the instrument, depending on its optical characteristics. A conversion is required.
A calibration set can be created of stars with well-known characteristics[2], using the responsivity of the camera and an estimate of the star's spectral density (the amount of emitted energy as function of the wavelength), based on the star's temperature according to Planck's law. The temperature can be obtained from the star's spectral class as listed in the most star catalogues. Interstellar extinction effects can be estimated assuming a magnitude correction.
With the help of the obtained calibration set, it is possible to plot for all stars available the magnitude shift against B-V and fit through these points a suitable polynomial, with a 1 σ error of 0.17 magnitude (Fig. 2.2).
If B-V for a catalogued star is unknown, it can also be estimated from its spectral class.

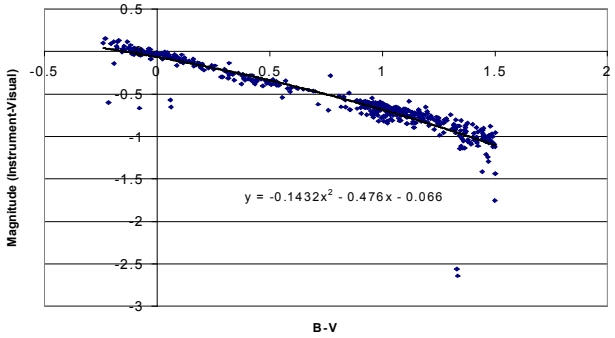

Fig. 2.2: Conversion from visual to instrumental magnitude by interpolation of calibration set.

2.1.2 Calculation of triangles

4 Ways have been implemented for star recognition by triangles: Quine, Liebe, Douma and DUDE:

Quine triangle: selects the brightest two stars within a certain radius from the base star [8].

Liebe, Douma and DUDE use the *same* strategy for extracting triangles from the CCD image: they take the closest neighbors for any detected star. However, a priori, because of the interference effects of camera noise, it cannot be *predicted* which stars exactly will appear in the images as neighbors of a certain base star. The three algorithms differ in the way that possible 'closest neighbor'-triangles are selected for storage in the database and in the way the right triangle (if available) is retrieved from the database.

Liebe triangle: stores all conceivable triangles that could be used for identification of the brightest stars in the sky in the database [1].
Douma triangle: Douma [6] has stored only the *'most likely'* one for each base star to save considerably on database size. From the estimated instrumental star magnitude the probability is estimated that a star is bright enough to be observed by the camera. The Liebe triangle with the highest probability is selected for the database.
DUDE triangle: This extended Douma algorithm closes the gap between Liebe and Douma and adds a number of refinements and additional features, most importantly:

- It uses probability margins to accept or reject a triangle. A single star has a controlled number of

triangles stored for recognition. Triangles that have too low a probability are rejected.

- DUDE takes into account the geometric effect of the relative positions of the neighboring stars and the limited size of the Field Of View (FOV). In general, likeliness of triangles with two distant neighbors and an angle between them close to 180 degrees is severely reduced, all in all accounting for about 10% of the database: they are unlikely to fit in the FOV.
- DUDE includes a model for optical binaries. For a camera with deliberately defocused star images with angular size of ~0.1° of arc, 5-10% of the stars is apparently clustered in indistinguishable groups. As a camera cannot distinguish between them, also the database should take them into account as single stars, with averaged position and combined magnitude.

2.1.3 Uniformization of the triangle set

When the triangles have been determined, they are stored in a database that is optimized for direct retrieval.

A logarithmic feature search in case of 4096 entries (=2^{12}) would have to compare 12 values before a target is found, and it can only treat one feature at the time.

The DUDE method for data storage is to use a 'pointer array'. The whole possible range of a certain triangle feature, say *distance A* (Fig. 2.1), is divided into a number of intervals, each part holding a pointer into a 'candidate array' of pointer lines, of which the entries point into the datalines of all candidates in yet another file (Fig. 2.2).

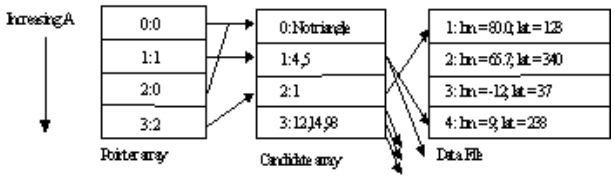

Fig. 2.2: 1D Pointer based data storage

A candidate is searched for within the expected error range from the measured value.

The distribution of the A-values and of the triangle features in general is not homogenous (Fig. 2.3). The interval range assigned to each individual 'pointer array' element can be sized by an estimator function such that the distribution is uniformized and thus data entropy is maximized. Each candidate array will hold an equal number of candidates. A uniform distribution guarantees minimal memory and processing effort for selection of the right candidate. The described process is called *uniformization* of the database (Fig. 2.4).

The 'pointer array' can also be 2 or 3 dimensional, with e.g. feature B in the second dimension etc.

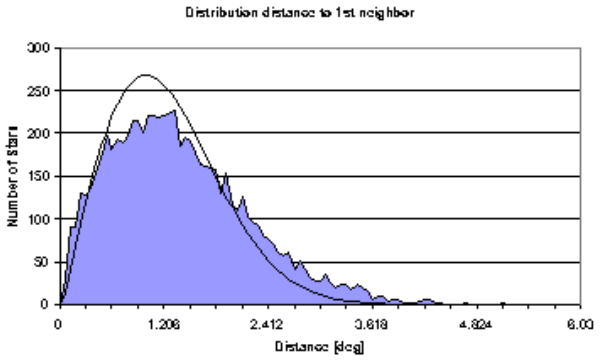

Fig. 2.3: Triangle feature A distribution including analytical approximation (See [Ref. 2])

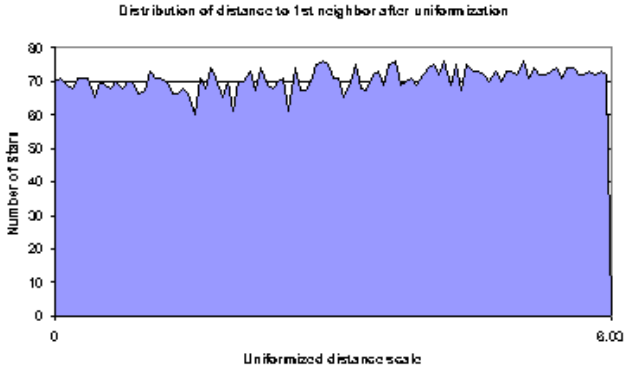

Fig. 2.4: Uniformized triangle distribution of A.

2.2 Detection and Centroiding

When real or synthetic[2] images (pixel maps) are used as input, bright pixel groups need to be detected and qualified as stars or rejected as false source. Then a centroiding algorithm is necessary to determine the position of the stars in the image at subpixel accuracy.

In principle the detection of stars can be done in hardware through the use of preprogrammed FPGAs, but more generally, for low cost sensors, the 'Lost In Space' problem will be solved in software.

The SSATT detection module finds stars by scanning stepwise through the pixel map. Pixels found to be below a certain detection threshold are ignored. If a pixel is found that is bright enough, its immediate surroundings are scanned. Then there are several possibilities:

The pixel is part of a bright pixel group and regarded as a star. The brightest pixel in the immediate neighborhood is localized. Centroiding is performed by computation of the 'center of gravity' in a fixed area of e.g. 3x3 pixels around the brightest pixel. Here noise effects are taken into account This noise has been found to be dependent on the actual pixel intensity and is interpolated from a calibrated table.

Some pixels are blooming. In this case, the brightest pixel is determined from investigation of the surrounding pixels. For increased centroiding accuracy, the total 'bloomed energy' is redistributed by an estimator function. The star is marked unreliable.

There are not enough bright pixels around to make up a reliable star. The star is rejected.
A large area is bloomed. The area is ignored.

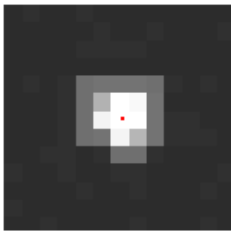

Fig. 2.5: Star in real image and centroiding result (indicated by dot).

After centroiding, the coordinates of the stars have to be transferred from a pixel cartesian frame to a frame for spherical angles to find and calculate the triangle features. This transformation is simple enough for an ideal lens, but is dependent on the lens imperfection. A parameterized model for these imperfections is determined. Although typically done through calibration with a point light-source, such a model can also be determined without physical measuring equipment. SSATT support S/W performs a semi-automatic genetic algorithm optimization using star-sky images only, by minimization of the summed squared errors of all the distances between detected stars (assuming their true distance is known from the database). This optimization yields a typical model for the lens projection imperfections such as Fig. 3.8.

2.3 Identification & Validation

A triangle is taken from the centroided image by a 'spiral' algorithm, a search algorithm that spirals out from a base star in the image to find the neighboring star positions. The selected descriptive features (Fig. 2.1) of the triangle are calculated.
The pointer array of the database is used to find the triangle candidates whose features fit within the estimated error range. Then, the candidate triangles pass through the *prevalidation*: a user defined filter that is a further check of a third or further triangle feature. Validation is performed afterwards through comparison of the individual distances between the identified stars as well as by a recursive process that is designed to increase the fraction of recognized stars while saving computing time.

Recursive identification
The recursive process uses the information of the neighbors of a validated star as a means of identification and further validation [2]: once a star has been identified through recognition of its triangle and validated with distance against a second –and unrelated- star, the identity of its neighbors in the triangle can be recovered from a neighbors-database without further calculations. If a matching candidate triangle is also available for at least one of these secondarily identified stars, its own neighbors within this triangle can be extracted straight from the neighbors-database, and so on. In this way, a single validation of distance between two stars can result in identification of a large part of the star field in the image without any further calculations.

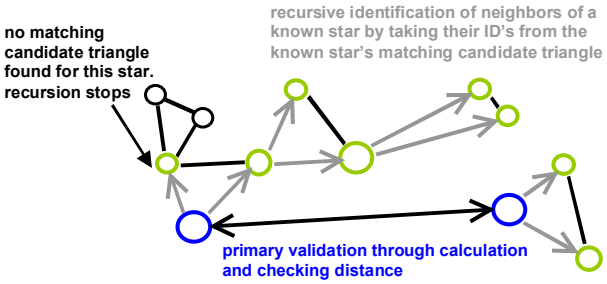

Fig. 2.6: Recursive identification of DUDE: from the calculation of a single validation distance between 2 remote stars in the image, 10 stars are reliably identified.

2.4 Attitude determination

The performance of the algorithms is assessed by attitude accuracy following from the QUEST (Quaternion Estimator) method [4,5]. Stars that have been tagged unreliable (centroided star groups, weak stars, blooming stars, stars near the edge) are taken into account at appropriate weighting. Extra robustness with respect to individual off-stars (poorly centroided) can be added by performing QUEST on several small subgroups of the identified stars and selecting the (weighted) median solution.

3. Test Results

After initial testing on sky images available from the web, 2 kinds of organized tests were performed:

- Simulations
  - Attitude reconstruction of synthetic star-sky pixel maps including simulated noise
  - Monte Carlo simulations for comparison with between different algorithms and for different cameras
- Automated batch processing of real-sky imagery

3.1 Simulation results

Simulations with synthetic images provided by TNO-TPD[2] show that with a relatively small database (240 kB) a very large fraction of all stars in the images is identified (over 80%). Attitude reconstruction accuracy is about 1/3 of the centroiding accuracy, comparable to e.g. the Van Bezooijen algorithm[7]. With comparable database size, a factor 3 improvement on accuracy is possible.
Monte Carlo simulations using the DUDE and other algorithms were performed for:

1. A 30x40 deg FOV commercial technology (e.g. CMOS) camera, 70 kB triangle database.
2. A typical 15x20 deg new generation star sensor (current industrial standard).

These tests are described in more detail in [Ref 2,3], so only an overview of the results is provided here.

Accuracy	15.6 arcsec
Reliability	100.0 %
Fraction of images rejected	11.6 %
Number of stars per image	9.8
Fraction of stars identified	78.7 %

Table 3.1: Commercial camera results with 70 kB database

	Mem [kB]	entries	acc arcs	reliab	succ	succ ID
DUDE	229	9017	1.3	100.00	100.00	82
DUDEhigh acc	542	31480	1.2	100.00	100.00	92.8
DUDElowmem	86	6036	2.3	100.00	98.5	63
Douma	147	6275	1.9	100.00	99.7	54.3
Liebe/DUDE	268	13402	1.2	99.8	99.1	22.6
Quine/DUDE	199	8669	1.4	100.00	99.9	45.8

Table 3.2: Summary of different algorithms for the Lost In Space problem using new generation medium cost star sensor technology. Succ = fraction of images that is not rejected. Succ ID = fraction of stars that is identified.

A summary of results is given in above tables. In table 3.1 it is shown that a commercial camera can be both very reliable and accurate, with a very low memory requirement. The only disadvantage is the fact that a significant fraction of the images (about 1 in 9) is rejected (too little reliable stars in the FOV). In practice, for nadir oriented spacecraft, this will mean that the camera will need more time to perform a successful Lost In Space solution.
For the Monte Carlo simulation of the new generation camera, DUDE, Liebe and Quine triangle selection models were tested with the database search and storage method of DUDE. Table 3.2 gives the results.
DUDE itself performs well, with near perfect reliability and arcsecond accuracy, especially because it recognizes a very large fraction of the stars in the image, due to the recursive identification and the optimized triangle storage.

3.2 MEFIST II real sky tests

The MEFIST II star sensor camera is a development by TNO-TPD in Delft, The Netherlands (Figure 3.1). SSATT was used to investigate over a 1000 images, taken in the Negev desert on 5-6 July 2000 (Fig. 3.12). Latitude of the observation site was about 31 degrees. The camera was pointing zenith, so this is also the latitude of the starsky in the images. Celestial longitude ranged from ~270-320 degrees, increasing with time at 15 degrees/hour. This change in longitude due to rotation of the Earth could be accurately reconstructed from the attitude solutions of the series of images, taken at 15 s interval. At regular intervals (every 120 images) rotation of ~20 degrees was performed, total clockwise rotation varied from 3 to 84 degrees. Table 3.3 provides an overview of the cases studied.

Image case	*Number of images studied*
800-8, 4 rotations*	479
800-4, 1 rotation	109
400-4, 4 rotations	473
Rate 200-8 (3 deg/6 deg)	60
Moon 100-1, 500-2, 500-4, 800-2	43 (number available, a selection was studied)

Table 3.3: explanation of cases: 800-8, 4 rotations: Integration time **800** ms, programmable gain set to **8**. Camera was oriented to zenith, and rotated **4** times around boresight axis

Reference case was the 800 ms integration time, gain setting "8". This is theoretically the most sensitive case, and therefore possibly the most accurate. It should be noted that the integration time of 800 ms causes a blur of 10.4 arcsec, or 0.055 pixel (each pixel = 188 arcsec), which might degrad static performance a bit.
Effect of gain and integration time were to be studied from the other settings with abundant imagery: 800-4 and 400-4. Images were studied that were taken with the camera mounted on a pendulum, as a means of rate simulation. Finally some special attention was reserved for images with the moon in the FOV, to verify problemless centroiding in the presence of large amounts of noise.
The camera electronics have removed the majority of the dark current noise from the images, so the noise level on all images seems very low.

Figure 3.1 shows the positions of all reliably identified stars in the FOV of the camera combined for all 800-8 images giving an impression of the spatial coverage of the CCD that was taken into account for the various performance estimates. Individual stars generally appear on subsequent images at slightly shifted location, hence the "strikes" in the image. Fig 3.2 shows for the same settings and the same stars the spatial coverage over the celestial sky.

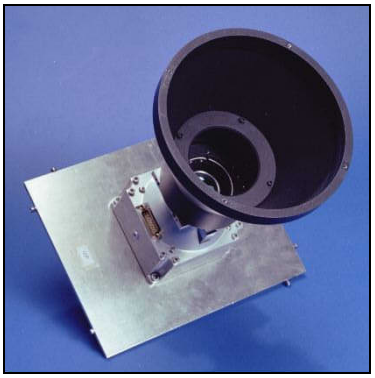

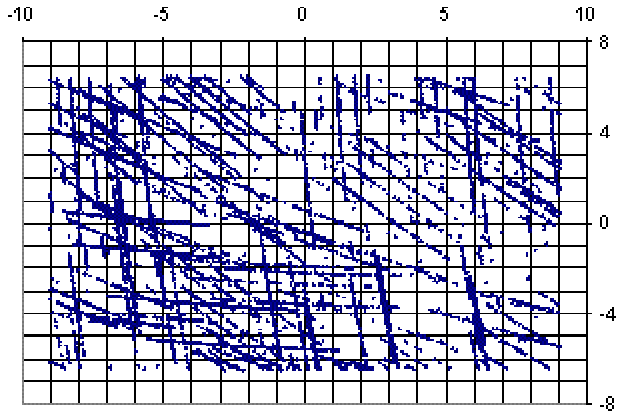

Figure 3.1: Above: MESIFT II. Below: position of all identified and accepted stars in the FOV of the camera combined for all 800-8 images. The apparent stripes indicate the shift of individual stars within the FOV, due to slow motion of the zenith (and camera) through the sky due ot rotation of the Earth. The Earth rotation could be calculated back with high precision from this data. Identified stars near the edge of the screen are rejected because they have higher likelihood of being false and have less precision due to projection of the lense.

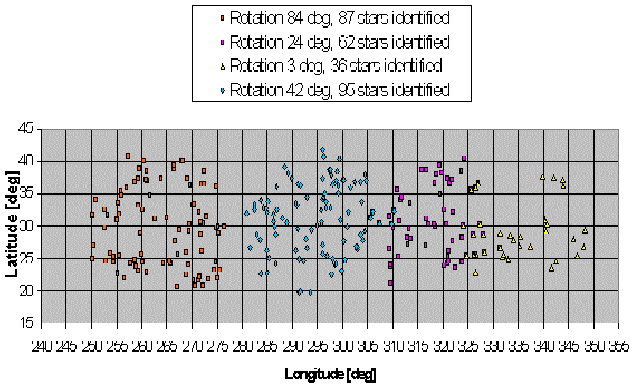

Figure 3.2: Position of the same identified stars as Fig. 3.1, but projected in the celestial sky. The four rotations are indicated by different colors. It will be shown in this paper that the observed reduction in stars identified with increasing longitude is due to reduction in bright star density in the sky.

3.2.1 Determining SSATT camera settings

In order to create an optimal triangle database for a specific camera, the magnitude threshold of the camera needs to be decided. This can be done by experimenting with the setting of the detection threshold for a star's max pixel value, and the number of pixels that is minimally required to build up a star. By using more pixels around the brightest one for each star, one can, to a certain limit, improve centroiding accuracy. The MEFIST is designed for a star spotsize of 3x3 pixels and indeed, the best centroiding results were obtained for about 9 pixels per star. Raising this number to 25 did not result in significant increase in number of identified stars. However, many stars will not be bright enough to light up 9 pixels above the threshold. Therefore, smaller star groups will also be accepted as potential stars.

In below figure 3.3, with 5-6 pixels required and a detection threshold for the brightest pixel value of a star of at least 23, it can be seen that the magnitude threshold should be put to about 6. About 60 stars per image will be found. If 4 pixels are accepted and a detection threshold of 7 pixel value, about 90 stars are found, the weakest of which will have a magnitude of ~6.7. If the detection threshold is set lower, groups of noise pixels surrounding singled-out bright pixels result in a significant number of false stars. Note one can indeed find in Fig. 3.3 that most stars light up about 8-9 pixels.

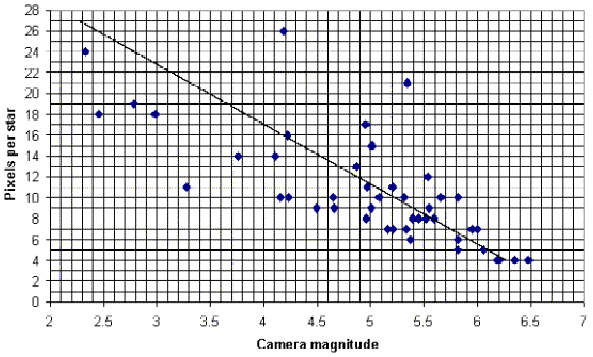

Figure 3.3: Relation between star size in pixels (above treshold) and camera magnitude. Data from 07052258.b00

The conclusion that most stars take up about 9 pixels is reinforced by studying

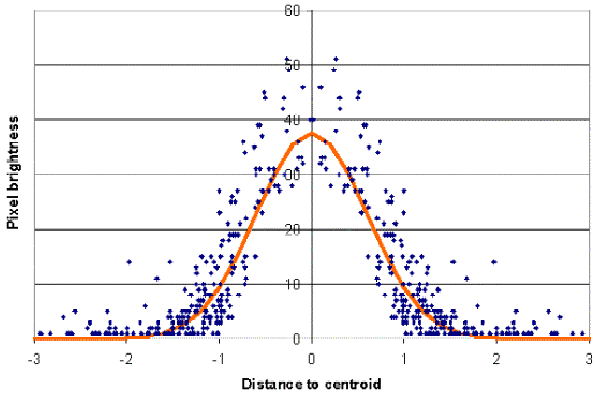

Figure 3.4. It shows the collected distances of pixel centers to the centroids of the stars they surround. It only includes the pixels from stars with a magnitude over 5.0. A nice Gaussian distribution is recognized for these most common (weak) stars. Their average projected size can be estimated to be of diameter ~3.5 pixel, again quite as expected, i.e. between the inner circle of a 3x3 pixel area (diameter 3) and its outer circle (diameter 4.2), therefore covering about 9 pixels in all.

Brighter stars do not quite follow this shape and there is evidence of blooming (bulging out of bright pixels at relatively large distance to the centroid; flat upper limits in pixel brightness can be distinguished representing local blooming limits). The bloom limits vary, between 150 and 220 (due to local-noise reduction by the camera hardware this value is not 255 as may be expected for a one-byte signal).

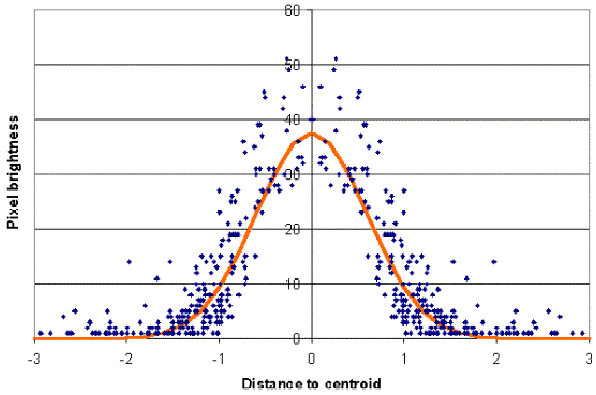

Figure 3.4 Distance of pixel center to centroid of star. Stars weaker than Magnitude 5. Data from 07052258.b00 (Red curve is a Gaussian curve with 1 sigma=0.6)

The identification performance of the SSATT algorithms was somewhat limited because only the Yale's Bright Star Catalogue was available, with 9096 stars complete to magnitude 6, rather than the camera's magnitude 6.7 established sensitivity. To match the catalogue, camera threshold was conservatively set to 5.7. The triangle-database-creation algorithm also needs the Centroiding Error (CE), which was found to be about ~40-55 arcsec. DUDE was the algorithm of choice.
During the star identification process the 2D-database is searched for candidate triangles with matching angles A and C (Fig. 2.1), before further validation is performed.

3.2.2 Magnitude reconstruction performance

Star magnitude is a logarithmic expression of brightness. Therefore, if all of a star's 9 pixelvalues are summed, it would ideally follow a straight line on a logarithmic plot, with slope -2.5. The offset is to be determined by a best fit of a line with such a slope. The observed data fits to a line of slope -2.17 (Fig. 3.5). The slight difference could have something to do with the clipping of pixel values by the noise reduction hardware inside the camera.

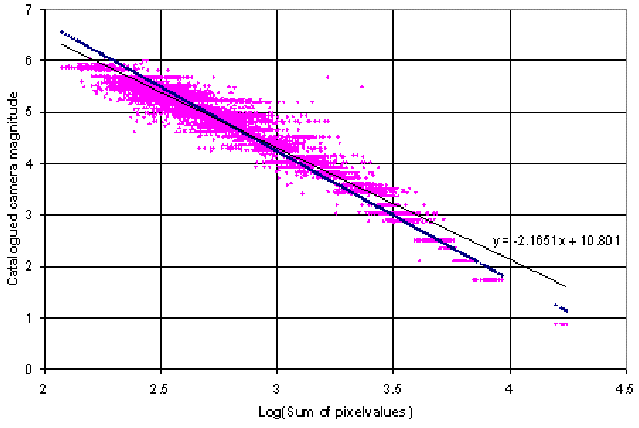

Figure 3.5: Logarithm of summation of an identified star's pixelvalue as a function of its catalogued camera magnitude. Two fits are shown, a best fit (slope –2.17) and a fit with enforced ideal slope (-2.5). The difference is not very significant but can be explained by the camera hardware functioning.

This process affects relatively more the pixel summation for weak stars than it does for bright ones, shifting stars with high magnitude more to the lower summations, in Fig. 3.5. Bright star magnitude could be underestimated due to blooming. Sticking to generality, a best fit with slope -2.5 was enforced.

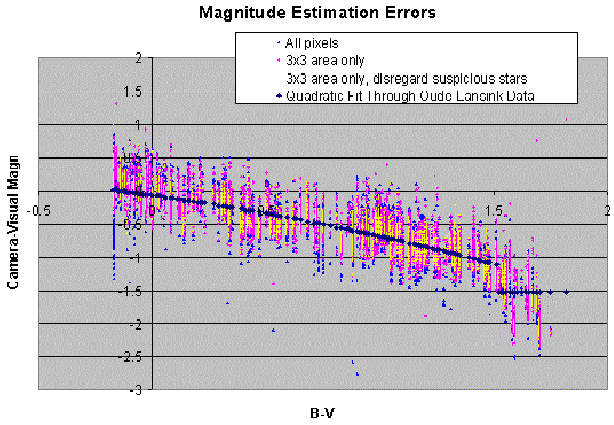

Figure 3.6: SSATT camera magnitude reconstruction of identified stars as compared to predictions from catalogue data (compare Fig. 2.2).

Remember that the catalogue only provides visual magnitudes. The conversion to camera magnitude for MEFIST was determined before the test from a calibration set by Oude-Lansink at TNO-TPD (Fig. 2.2).
Figure 3.6 shows how well the reconstruction of camera magnitudes from the pixel summations match Lansink's predicted quadratic curve. Star camera magnitudes can thus be well predicted based on the catalogued (visual) data. This allows for SSATT to create a near-optimal database, beneficial to identification performance:
the star magnitude noise affects the likelihood of certain triangles to occur. The 1 sigma magnitude error of Lansink's quadratic fit is 0.17 (Fig. 2.2). The final magnitude estimation noise during the real-sky test ranges from 0.2-0.23 for an assumed 3x3 pixel star size.

3.2.3 Lens adjustment model

To obtain the best possible attitude reconstruction, a 1-dimensional lens projection adjustment model was provided by TNO-TPD and included into the image-to-sky coordinate transformation[12]. We further detailed it, in 2D, using SSATT's optimization algorithm in the following manner.
20 Well-identified images were selected from the g8-i800 dataset, covering all 4 rotational angles and a representative selection of celestial longitudes. From each of these images, 15 stars were selected, all in all giving a more or less equally distributed coverage over the FOV or lens projection area (Figure 3.7). A cost function was set-up, adding all squared distance errors (difference between centroided and catalogued angular distance) between all possible pairs of selected stars within a single image. This cost was minimized through genetic algorithm optimization[11], in a variety of parameter ranges. A typical lens projection adjustment result is given in Figure 3.8. The genetic algorithms were run over a relatively small number of generations (1000), and considerable improvement might as yet be

possible. However, a consistent improvement in attitude performance (~40%) was already noticed.

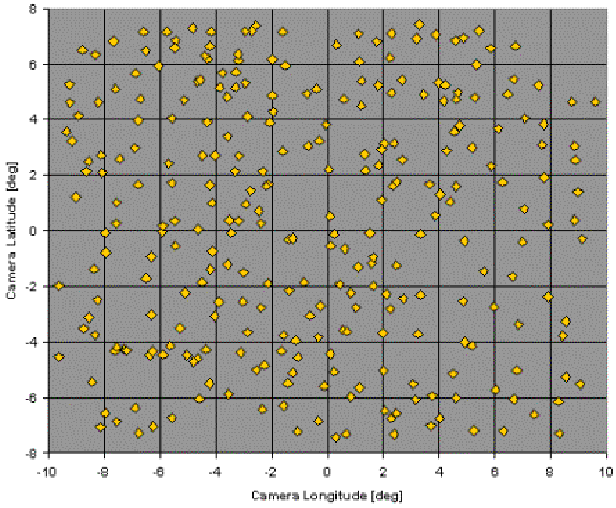

Figure 3.7: Position of selection of 300 reliably-identified stars in the FOV of the camera taken from 800-8 images. It was attempted to obtain a uniform distribution.

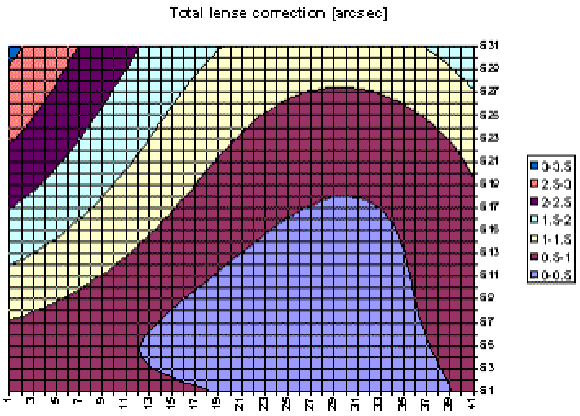

Figure 3.8: Magnitude of centroiding adjustments with respect to ideal lens, determined by Genetic Algorithms. The grid should be overlaid with the CCD surface. The axis numbering is in an awkward scale, derived from Excel column/row number, i.e. (half degrees+1) measured from the corner of the CCD.

3.2.4 Attitude reconstruction performance

As there is no reference attitude for the images two methods have been used to determine the attitude accuracy. The methods are referred to as the *latitude method* and the *cloud method*.

The latitude method is based on the principle that during a test (same setting, same rotation) the camera points straight up in the same direction and therefore the reconstructed latitude should stay constant. However due to atmospheric effects and possible tiny displacements of the tripod due to wind and or temperature effects this assumption is only valid within a few arc seconds accuracy. In some cases a clear and consistent drift was observed of the latitude direction of several arcsec per minute. It is also possible that this drift is due low frequency changes within the camera hardware, but due to lack of reference attitude, it is not possible to distinguish between these drifts. We have to limit ourselves to quantify the attitude reconstruction noise with respect to the momentary (unknown) offset. Drift effects are thus to be removed. We therefore fit a second order polynomial through the latitude deviations from the average reconstructed attitudes. To obtain a measure for the reconstruction accuracy, the deviation to this fit is multiplied by $\sqrt{2}$. This accounts for identical and independent error in longitude direction. In Fig. 3.9 an example is presented for the g4-i800 photo series. The blue dots represent the latitude deviation from the average reconstructed latitude in this photo series. Through these blue dots a trend-line is fitted. The quoted accuracy is 10.6 arcsec is $\sqrt{2}$ * the standard deviation around this trend.

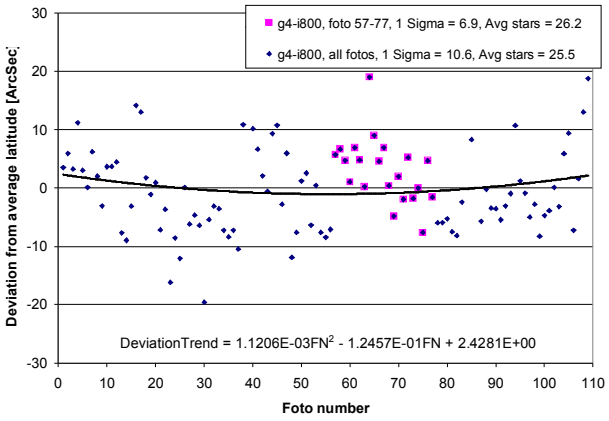

Fig. 3.9: Latitude method for attitude reconstruction. The actual camera orientation's latitude is assumed to change only slowly over time, as consecutive images are taken during the testing. Noise around the trendline can be interpreted as a way to determine the 1D-attitude reconstruction error. This simple method works surprisingly well.

The cloud method (Fig. 3.10) reconstruction accuracy is obtained by multiple attitude reconstructions of a selected image (bootstrap method). Each attitude reconstruction is performed with a different subset of identified stars, roughly representing the range of performance through out all the tests. The deviation of each reconstructed attitude with respect to the average attitude is then scaled to the average number of stars of the originally identified set. The scaling is performed in order to correct for the number of stars used for each attitude reconstruction. As the attitude reconstruction accuracy is inversely proportional to the square root of the number of stars used for the attitude reconstruction the applied scaling for each deviation equals $\sqrt{}$(number of stars used to reconstruct attitude)/ $\sqrt{}$(average number of stars of original identification). The standard deviation of these scaled errors is the measure for the reconstruction accuracy with the cloud method.

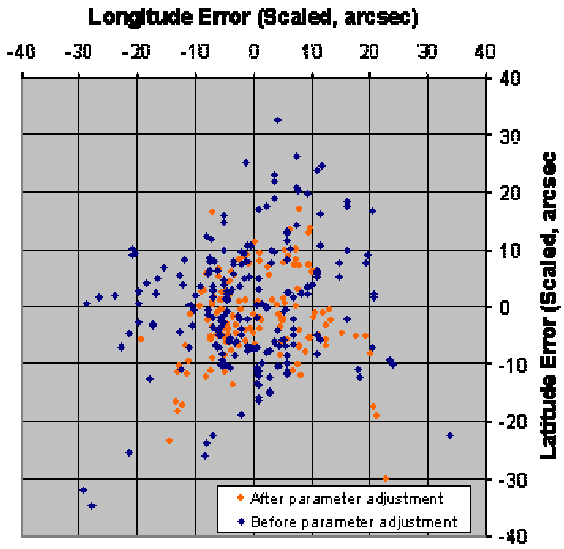

Fig. 3.10: Cloud method for attitude reconstruction. Attitude is reconstructed using different subsets of the set of identified stars for a certain image. The errors with respect to the average direction are plotted (bootstrap method). This method gives no insight into the offset, e.g. due to misalignments, but gives good insight into the standard deviation of the reconstruction. Two sets are plotted, the orange one is after parametric lens adjustment and significantly improves performance.

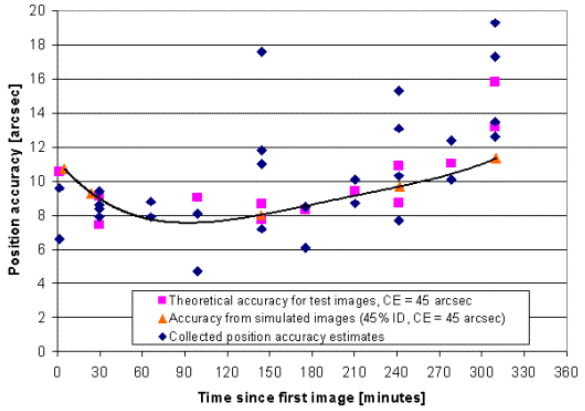

Fig. 3.11: Attitude reconstruction error estimates over time. The performance change with (test) time can be explained by the change of star density in the sky due to Earth rotation. See text for explanation.

Both methods give comparable results (the results combined are plotted with blue diamonds in Fig. 3.11). The number of stars in the sky changes due to rotation of the Earth. Therefore the obtainable accuracy changes with time, roughly according to *Centroiding Error / √ (0.45 x number of stars in simulated image)*. This formula takes into account that the average number of stars used for attitude determination with current settings is about 45% of the total amount of stars in the image. Whereas the blue diamonds indicate the combined estimates of the two methods using real-sky images, the pink squares are performance calculated with above formula, for the same number of stars that SSATT identified in the real-sky images. A centroiding error of 45 arcsec is assumed (0.24 pixel). We also created with SSATT fully simulated images for the same directions and let SSATT reconstruct attitude, assuming centroiding error of 45 arcsec. The curve (with red triangles) indicates the results.
Both theoretical results show the same trend as the results obtained by the test series, suggesting that the source of the tendency is merely the number of stars in FOV. The dominant effect of the number of stars on the attitude reconstruction error makes it impossible to determine effects of camera settings and or temperature effects.

In conclusion: attitude reconstruction precision for MEFIST II is thus found to be about 10 arcsec. Some improvements may be expected.
In space there will be no atmospheric noise & absorption/reflection effects, also extra precision may be gained by using a more complete star catalogue for the g8-i800 setting. Centroiding error can be improved: lens correction was not fully optimized (i.e. convergent), merely a general improvement of performance was achieved. Rotation of the Earth during the tests may have accounted for 5-10 arcsec contribution.

Note that we adopted in this document the term Attitude Reconstruction Precision (ARP) rather than the Noise Equivalent Angle (NEA). NEA is defined as[9]:
"The star tracker's ability to reproduce the same attitude when it is continously presented with the same star image. NEA is a nonsystematic, or random error component."
It is expected that the average of the ARP found by the two methods is a good representation of the NEA. In the definition of NEA, the ARP via the latitude method would give an upper limit of the NEA (because of the timeframe of 1 hour of a test series). On the other hand the cloud method would give a lower limit of the NEA because it is based on exactly the same camera image rather than the same star image.

3.2.5 Reliability of SSATT attitude reconstruction

Success is defined as: fraction of successfully identified images out of all images.
Reliability is defined as: fraction of successfull identified images out of all identified images.
Reliability is considered more important, since it is not so bad to skip a datapoint in a sequence of attitude estimations, but it is bad if an attitude is passed on, though wrong.

Reliability is always found to be 100%. False attitudes always have a warning tag (too little pixels, suspected double star, edge of screen etc.). In the way to deal with warning tags, we distinguish two options:

- Strict recognition
- Non-strict recognition

In case of a strict recognition (rejecting all stars with warning tag), only 0.2% of the images (i.e. one) yielded a wrong attitude, but it included a warning tag. 14 Images did not yield an attitude at all. So *success* for strict recognition can be estimated at 97%.

Non-strict recognition also rejects stars with warning tags, but allows them to participate if too little reliable stars are available. Images with only 3 identified stars are rejected no matter what. For non-strict recognition the *success* fraction is 99%. Reliability is still 100%.

Fig. 3.12 Installation of MEFIST on Wise Observatory, Negev desert.

4. Spin-off applications for SSATT

SSATT functionality has been demonstrated. Simulations indicate that the DUDE algorithm can be used even with commercial technology on the ground. This allows for use of the algorithms for various spin-off applications. This section provides an overview of the initial efforts we have made in this direction.

4.1 Telescope direction sensor for amateur astronomy

The star sensor attitude reconstruction S/W is to be provided as an off-line tool that runs on a laptop and is connected to a webcam, rigidly attached to the telescope. The tool will automatically process the images stored on the laptop by the webcam and produce the exact direction of the telescope. Contrary to more costly and work-intensive alternatives, the attitude reconstruction is independent of the telescope alignment or location. This will make easy and quick pointing affordable for most amateur astronomers. Current equal performance alternatives for this group are more costly GPS based systems.

The required adjustments to the "Space Version" are:

- Creation of simpler user input interface oriented at typical web-cam parameters that are easy to enter by amateurs (number of pixels, width of camera image). Fixation of many advanced variables and options in the tool.
- Automated conversion of user input into standard S/W parameters (focal length, field of view etc.).
- Internal setting of parameters for wide range of typical web-cam type cameras (sensitivity vs. light frequency etc.).
- Addition of filter against stray-light and web-cam image compression effects. Automated noise level and threshold detection.
- Automated processing of incoming webcam images
- Large display of attitude result
- Simplified user manual

In co-operation and exchange with the German astronomer community, some web-cam sky imagery was studied. It turns out that reasonably high-grade cameras with long integration times are required. The market for this product is nevertheless judged a considerable part of the amateur astronomy, because of the simplicity and low projected added cost of the product, relatively small additional investment required (if digital camera and laptop are available) and clear benefit to the observer.

A more advanced software system could contain a direct link with the web-cam (so drivers are required) and an astronomical target database and ephemeris. The program would ask the observer for a requested target and provide steering information (such as "left, right, up, down"). Based on a preliminary market study performed in co-operation within the European LOSTESC program we judge the expected increase of market small considering the extra effort required. Also a complete, embedded system -without need for additional hardware- for scientifically-inclined high school children was studied in this context but judged not feasible because of too high production cost of such devices.

4.2 Meteorite & satellite observation, identification and logging for amateur astronomers

Delta-Utec has been approached by the Leiden astronomers' group to develop a tool, similar to that mentioned above, but for higher performance cameras, with the added feature of a user interface that allows marking of meteorite-stripes within the image and subsequent automated calculation and logging of their direction.

This application requires only minor changes with respect to the "Space Version":

- Extensive Hipparcos database as input for the tool, to allow for more sensitive cameras and smaller field of view.
- User input or automated option for marking of starting and endpoints of meteorite stripes in the image.
- Calculation and logging of stripe vector based on attitude of image and location of stripe within image.

An Italian group requested a similar capability, namely for marking stripes created by passing satellites. We believe exactly the same tool can be used for both applications. The log-file can be connected to post-processing software that will then produce the Two-Line Elements for the observed satellites.

4.3 Database search algorithm

The "multidimensional uniform" database search structure developed by Delta-Utec for the star pattern recognition has already been transferred to an orthopedic database application with a very significant gain in search time of a factor 100, thus significantly improving the company's edge with respect to its competitors.

It has thus been shown that this fast structure can be implemented in Earth applications, e.g. face pattern recognition algorithms for automatic detection of wanted persons from security camera images (which are using a similar triangle based strategy). The database search structure can be prepared such that the beneficiaries' S/W developers can easily implement the same method in a wide range of Earthly applications.

4.4 Other SSATT spin-offs

4.4.1 Attitude test-bed reference

In a direct ground-based application of SSATT, a star sensor coupled to our software was proposed for use for reference measurements for a GPS-attitude test bed by Aalborg University. A successful test with real sky imagery of the camera hardware was performed, but the project was halted because of unrelated reasons.

4.4.2 Military applications

SSATT has been considered by the Dutch military for use with a camera on F16 fighters to reset gyroscope IMUs during long-duration night flights. The project was halted for unknown reasons.

5 Conclusions

Through simulations and real-sky tests, it has been demonstrated that the Star Sensor & Algorithm Test Tool (SSATT), using the DUDE algorithms can be used to provide attitude reconstruction for CCD images with ~5-10 arcsec accuracy and 100% reliability, on ground, as well as, expectedly, in space. Embedded software for such applications has been created and is available.

Originally developed to support development and assess performance of star sensor cameras and algorithms, SSATT can now be used to batch-process large quantities of real-sky images. In particular in this paper, the MEFIST II camera real-sky test results have been described.

These tests create a firm basis for a number of spin-off possibilities which have been investigated and/or described in various levels of detail, including also the DUDE database search strategy, which was successfully implemented in a medical application.

Acknowledgments

The MEFIST-II testing was performed under Dutch NRT-2802T funding with TNO-TPD, with support of University of Tel Aviv and Asher Space Research Institute (ASRI), from the Technion University in Haifa. Spin-off investigations & discussions were performed in co-operation with Joerg Hoebelmann (amateur astronomer), Thomas Bak (Aalborg University), Benoit Mintiens (LOSTESC), Marti b.v. (orthopedic S/W), Joe Zender (meteorites), Prof. Filippo Graziani, Fabrizio Piergentili, La Sapienza (satellite logging), Martin v.d. Pol (MartinSpace, Dutch Airforce).

References

[1] Liebe, C.C., "Star Trackers for Attitude Determination", IEEE AES Systems Magazine, June 1995.

[2] Heide, E.J., Kruijff, M., Oude-Lansink, D., Douma, S., Development and Validation of a Fast and Reliable Star Sensor Algorithm with Reduced Database, IAF-98.A.6.05, available from www.delta-utec.com.

[3] Zuiderwijk, S., Kruijff, M., Heide, E.J. v.d., "SSATT: A Tool for Automated Evaluation of Star Sensor Design, Performance and On-Board Algorithms". 4th ESA International Conference on Spacecraft Guidance, Navigation and Control Systems, ESTEC[i]. , Noordwijk, 18-21 October 1999, ESA-SP-425, February 2000

[4] Shuster & Oh, Three Axis Determination from Vector Observations, JGC, AIAA81-4003

[5] Bar-Itzhack, I.Y., "REQUEST: A Recursive QUEST Algorithm for Sequential Attitude Determination", AIAA Vol 19, Number 5, pages 1034-1038

[6] Douma, S.R., "Development of an Algorithm for Autonomous Star Identification", Delft University of Technology, Faculty of Aerospace Engineering, 1997

[7] Bezooijen, R.W.H., "Automated Star Pattern Recognition", PhD Stanford University, California 1989

[8] Quine, B.M., Durrant-Whyte, H.F., "A fast autonomous star acquisition algorithm for spacecraft, In proceeding of IFAC Autonomous Control Conference", Beijing, 1995

[9] Eisenman, A, Liebe, C.C, The advancing State-of-the-Art in Second Generation Star Trackers, JPL

[10] Zuiderwijk, S., The Star Sensor Control Unit, An embedded solution for autonomous attitude determination, Hogeschool van Utrecht/Delta-Utec, May 2000.

[11] Biesbroek, R., Evolution in a Micro-Chip, A Brief Study into Genetic Algorithms ESA/ESTEC working paper, E.W.P. 1870, 1996.

[12] Heiden, N. v.d., TNO TPD Medium Field Star Tracker (MEFIST) performance. TPD-NRT-MEFIST-TN-01, June 2000

[13] M. Kruijff, E.J. van der Heide, Image Processing for MEFIST Real Sky Test Negev Desert - July 2000. Delta Utec, May 2001.